NUWC-NPT Technical Document 10,883
9 May 1995

High-Power Terfenol-D Flextensional Transducer

A Paper Presented at the Office of Naval Research Transducer Materials and Transducers Workshop, Pennsylvania State University, University Park, Pennsylvania, 4 April 1995

Mark B. Moffett
Environmental Tactical Support
Systems Department

Raymond Porzio
Gerald L. Bernier
Lockheed Sanders, Incorporated

Naval Undersea Warfare Center Division
Newport, Rhode Island

PREFACE

The work presented in this document was sponsored by the Office of Naval Research (ONR) and was presented on 4 April 1995 at the ONR Transducer Materials and Transducers Workshop held at the Pennsylvania State University, University Park, Pennsylvania.

Reviewed and Approved: 9 May 1995

B. F. Cole
Head, Environmental and Tactical Support
Systems Department

REPORT DOCUMENTATION PAGE

Form Approved
OMB No. 0704-0188

1. AGENCY USE ONLY (Leave Blank)	2. REPORT DATE	3. REPORT TYPE AND DATES COVERED
	9 May 1995	Final

4. TITLE AND SUBTITLE

High-Power Terfenol-D Flextensional Transducer

5. FUNDING NUMBERS

PR H60025

6. AUTHOR(S)

Mark B. Moffett, Raymond Porzio (Lockheed Sanders) and
Gerald L. Bernier (Lockheed Sanders)

7. PERFORMING ORGANIZATION NAME(S) AND ADDRESS(ES)

Naval Undersea Warfare Center Detachment
39 Smith Street
New London, Connecticut 06320-5594

8. PERFORMING ORGANIZATION REPORT NUMBER

TD 10,883

9. SPONSORING/MONITORING AGENCY NAME(S) AND ADDRESS(ES)

Office of Naval Research
800 N. Quincy Street
Arlington, VA 22217-5000

10. SPONSORING/MONITORING AGENCY REPORT NUMBER

11. SUPPLEMENTARY NOTES

A paper presented at the Office of Naval Research Transducer Materials and Transducers Workshop, Pennsylvania State University, University Park, Pennsylvania, 4 April 1995.

12a. DISTRIBUTION/AVAILABILITY STATEMENT

Approved for public release; distribution is unlimited.

12b. DISTRIBUTION CODE

13. ABSTRACT (Maximum 200 words)

A flextensional underwater acoustic projector, powered by Terfenol-D and operated at a depth of 400 ft (122 m), has been driven to a source level of 212 dB//μPa-m at the Naval Undersea Warfare Center's (NUWC) Seneca Lake Test Facility. The flextensional shell was a modified Class IV shape having concave, rather than convex, radiating surfaces. The geometry of the shell was similar to one described by Merchant [U. S. Patent No. 3,258,738, June 28, 1966]. The shell cross-section was circumscribed by a rectangular area 9.8 x 5.0 inches (250 mm x 126 mm), and the height between the end flanges was 5.8 inches (148 mm). At the resonance frequency of 930 Hz, the projector was omnidirectional, and so the radiated acoustic power was 14 kW. The ac efficiency was 52 percent, and the overall (ac + dc) efficiency was 45 percent. The mass of the transducer was 34 lbm (15.4 kg). With a mechanical quality factor, Q_m, of 4.7, the projector figure-of-merit exceeded 200 W/kg-kHz-Q. The effective coupling factor, measured with the transducer in air, was 0.29.

14. SUBJECT TERMS

Flextensional Transducer
Transducers

15. NUMBER OF PAGES
22

16. PRICE CODE

17. SECURITY CLASSIFICATION OF REPORT	18. SECURITY CLASSIFICATION OF THIS PAGE	19. SECURITY CLASSIFICATION OF ABSTRACT	20. LIMITATION OF ABSTRACT
Unclassified	Unclassified	Unclassified	SAR

HIGH-POWER TERFENOL-D FLEXTENSIONAL TRANSDUCER*

MARK B. MOFFETT
New London Detachment, Naval Undersea Warfare Center
Fort Trumbull, New London, CT 06320-5594

RAYMOND PORZIO and GERALD L. BERNIER
Antisubmarine Warfare Directorate, Lockheed Sanders, Inc.
P. O. Box 868, Nashua, NH 03061-0868

ABSTRACT

A flextensional underwater acoustic projector, powered by Terfenol-D and operated at a depth of 400 ft (122 m), has been driven to a source level of 212 dB//μPa-m at the Naval Undersea Warfare Center's (NUWC) Seneca Lake Test Facility. The flextensional shell was a modified Class IV shape having concave, rather than convex, radiating surfaces. The geometry of the shell was similar to one described by Merchant [U. S. Patent No. 3,258,738, June 28, 1966]. The shell cross-section was circumscribed by a rectangular area 9.8 x 5.0 inches (250 mm x 126 mm), and the height between the end flanges was 5.8 inches (148 mm). At the resonance frequency of 930 Hz, the projector was omnidirectional, and so the radiated acoustic power was 14 kW. The ac efficiency was 52 percent, and the overall (ac + dc) efficiency was 45 percent. The mass of the transducer was 34 lbm (15.4 kg). With a mechanical quality factor, Q_m, of 4.7, the projector figure-of-merit exceeded 200 W/kg-kHz-Q. The effective coupling factor, measured with the transducer in air, was 0.29. [Work sponsored by the Office of Naval Research (ONR).]

INTRODUCTION

Flextensional transducers driven by stacks of PZT plates or rings have been widely used as low-frequency, high-power, underwater acoustic projectors.[1] The most common form of flextensional transducer is the Class IV (Royster's nomenclature[2]) oval shape, whose radiating surface is an elliptical cylinder. In the radiating mode and under hydrostatic pressure, the convex surfaces at the ends of the minor axis move out of phase with the ends of the major axis of the ellipse. Thus, as the transducer is operated at greater depths, the hydrostatic pressure increase tends to reduce the amount of compressive prestress applied to the extensional driver. This, in turn, means that the danger of overstressing the driver increases with the depth of operation. To ensure that such projectors maintain adequate prestress for their operation at depth, a large prestress must be applied to the driver stacks during construction. Studies[3] of PZT-8 stacks indicate that depolarization can result from the continued application of very high prestress.

---

*A paper presented at the ONR Transducer Materials and Transducers Workshop, Pennsylvania State University, University Park, Pennsylvania, 4 April 1995.

The opposite behavior occurs if the radiating surfaces are concave, rather than convex. A 1966 patent by Merchant[4] describes an underwater flextensional projector with concave surfaces. In this configuration, the extensional motion of the driver stack is in phase with the radiating surface, and the compressive prestress applied to the driver stacks increases with increasing hydrostatic pressure. Therefore, this type of projector, denoted as Class VII by Rynne,[5] should be capable of producing larger source levels at greater depth, where the increased cavitation threshold allows cavitation-free operation to higher levels. Furthermore the prestress applied to the stacks or rods during construction can be a moderate value, say 2000 psi, so that deterioration will not occur during storage.

Terfenol-D ($Tb_{0.3}Dy_{0.7}Fe_{1.93}$) is a highly magnetostrictive alloy whose superiority to piezoelectric PZT as a high power transducer drive material is well known,[6-9] but successful demonstrations of its practicality in a flextensional underwater projector have heretofore been lacking. For example, Terfenol barrel-stave flextensional projectors built and tested at NUWC have suffered from low efficiency and low coupling factor because of insufficient space for an efficient magnetic return circuit.[9,10] In this paper, we describe a Class VII, Terfenol-D flextensional transducer that overcomes those previous limitations.

I. THEORY

The electromechanical equivalent circuit for flextensional transducers is complicated by the presence of multiple modes of radiation. The intended mode is, of course, a flexural mode in which the transducer shell bends at a relatively low resonance frequency. Also present, however, is a "breathing" mode in which the shell expands and contracts extensionally at a higher resonance frequency (typically about 3 times the fundamental, flexural resonance). The breathing mode usually involves a higher coupling factor, and is more efficient than the flexural mode, and so its presence can have a significant effect on the equivalent circuit parameters used to describe the fundamental, flexural mode. One solution to this problem is to include the breathing mode in a multi-resonator equivalent circuit.[11-13] This approach has some merit in design studies, because reasonable estimates of the circuit elements can often be made from first principles. However, the large number of circuit parameters renders experimental verification almost impossible, because there are more of them than there are independent transducer quantities that can be accurately measured.

An alternative approach to the development of an equivalent circuit is the traditional one,[14] adopted herein, in which the canonical equivalent circuit of Van Dyke,[15] is chosen. With this method, it is possible to measure all the parameters for the equivalent circuit, but they tend to be *ad hoc* in nature, at least, for flextensional transducers. (Because we can relate the circuit elements of the canonical equivalent circuit to those of the more complex, multi-mode circuit, we still hope to be able to draw certain conclusions from the measured behavior of the transducer, however.) The canonical circuit is only valid in the neighborhood of the fundamental resonance, but that is, of course, where the transducer description is most important to us.

Figure 1 is the canonical equivalent circuit for magnetic-field transducers. Figure 1a shows the mechanical loop explicitly as a mechanical impedance analogy, with velocity analogous to current and force proportional to voltage. The velocity we choose as the modal reference[16] velocity for the present purposes, V, is the spatial average value (i. e., averaged over the radiating surface of the transducer). Then the acoustic volume velocity is simply the product

VA, where A is the active, radiating area. With V taken as the spatial average velocity, the radiation resistance for an omnidirectional projector at low frequencies is[17]

$$R_r = \pi\rho A^2 f^2/c\,, \tag{1}$$

where ρ is the density of the acoustic medium, c its sound speed, and f is the frequency. The mechanical loss resistance, R_m, can be related to R_r through the mechano-acoustic efficiency,

$$\eta_{ma} = R_r/(R_r + R_m)\,. \tag{2}$$

The mass, M, in Fig. 1a, is the modal mass of the transducer. It can be related to the mechanical quality factor, Q_m, through the relationship

$$Q_m = 2\pi f_0 M/(R_r + R_m)\,, \tag{3}$$

where f_0 is the open-circuit, mechanical resonance frequency. The resonance frequency is determined by the mass, M, and the open-circuit compliance, $C_m{}^I$, as

$$f_0 = [2\pi(MC_m{}^I)^{1/2}]^{-1}\,. \tag{4}$$

The electromechanical gyrator of Fig. 1a is the magnetostrictive analog of the electromechanical transformer that occurs in piezoelectric transducers.[18] (The electromechanical transformer converts the applied voltage, E to a blocked force, $F_b = NE$, where N is the electromechanical turns ratio of a piezoelectric transducer.) The electromechanical gyrator converts the applied current, I, to the blocked force,

$$F_b = \gamma I\,, \tag{5}$$

where γ is the electromechanical gyrator ratio, while the voltage across the gyrator electrical side is γV. When the motion of the transducer is blocked, $V = 0$, and the electrical side of the gyrator appears as a short circuit. When the transducer is electrically open, i. e., when $I = 0$, the mechanical side of the gyrator appears as a mechanical short-circuit. The gyrator converts a mechanical impedance, Z_m, on its mechanical side to an equivalent electrical impedance,

$$Z_e = \gamma^2/Z_m\,, \tag{6}$$

on its electrical side.

In Fig. 1a, the elements on the electrical side of the gyrator are the blocked inductance, L_b, and the blocked resistance, R_b. These blocked elements also appear in the purely electrical equivalent circuit of Fig. 1b, where the electromechanical gyrator and the mechanical branch have been replaced by a parallel electrical circuit with motional inductance, L_m, motional capacitance, C_m, and motional conductances, G_m and G_r. The motional inductance, by virtue of Eq. (6), is

$$L_m = \gamma^2 C_m{}^I\,, \tag{7}$$

i. e., proportional to the open-circuit mechanical compliance, C_m^I. Similarly, the motional capacitance is

$$C_m = M/\gamma^2 , \tag{8}$$

i. e., proportional to the modal mass, M. Again, through the use of Eq. (6), we obtain

$$G_m = R_m/\gamma^2 , \tag{9}$$

and

$$G_r = R_r/\gamma^2 , \tag{10}$$

so that the motional mechanical-loss and radiation conductances of Fig. 1b are directly proportional to the mechanical-loss and radiation resistances, respectively, of Fig. 1a.

Substitution of Eqs. (9) and (10) into Eq. (2) yields

$$\eta_{ma} = G_r/(G_r + G_m) . \tag{11}$$

and use of Eqs. (8)-(10) in Eq. (3) gives

$$G_r + G_m = 2\pi f_0 C_m/Q_m . \tag{12}$$

Analysis of the equivalent circuit of Fig. 1b at the resonance frequency,

$$f_0 = [2\pi(L_m C_m)^{1/2}]^{-1} , \tag{13}$$

shows that the reactance at f_0 is

$$X(f_0) = 2\pi f_0 L_b , \tag{14}$$

and the resistance is

$$R(f_0) = R_b + (G_r + G_m)^{-1} . \tag{15}$$

The electromechanical efficiency is

$$\eta_{em} = [1 + R_b(G_r + G_m)]^{-1} , \tag{16}$$

and the overall, ac, electroacoustic efficiency is

$$\eta_{ea} = \eta_{em}\,\eta_{ma} . \tag{17}$$

The motional and blocked inductances are related in terms of the effective coupling factor, k, of the transducer through the relationship

$$k^2 = L_m/(L_m + L_b)\,. \qquad (18)$$

The coupling factor is a measure of the bandwidth over which the transducer can be impedance-matched to a power amplifier.[19] Methods for its measurement were discussed by Woollett.[14]

We can obtain all six equivalent circuit parameters of Fig. 1b through a series of measurements of the transducer properties at and near resonance in water, with one exception. We will need to evaluate the effective coupling factor via measurements in air, because the quality factor, Q_m, for water loading is not large enough to allow an accurate determination[14] of k. The other five parameters to be measured in water are the resonance frequency, f_0, the mechanical quality factor, Q_m, the reactance, $X(f_0)$, the resistance, $R(f_0)$, and the electroacoustic efficiency, η_{ea}. To derive the circuit elements of Fig. 1a, we use Eq. (1) to evaluate the radiation resistance, R_r, and Eq. (10) to obtain the electromechanical gyrator ratio, γ. Then, the remaining three mechanical elements, C_m^I, M, and R_m, are obtained via Eqs. (7), (8), and (9), respectively.

II. EXPERIMENT

Figure 2a is a photograph of the partially assembled Terfenol-D flextensional transducer, and Fig. 2b shows the completed projector. In the center of Fig. 2a can be seen the four drive coils, which are electrically connected in parallel. Each coil is 2.72 inches (69.0 mm) in axial length and consists of 489 turns of AWG #18 magnet wire. The magnetic field circulates in the counterclockwise direction indicated by the arrows. Largely hidden by the coils are the four Terfenol-D rods, each of length 2.93 inches (74.3 mm) and diameter 1.30 inches (33.0 mm). The Terfenol-D was laminated with 0.14-inch (3.6-mm) laminations to minimize eddy-current losses within the rods. The Terfenol-D rods were manufactured and laminated by Etrema Products (a subsidiary of Edge Technologies) of Ames, IA. Completing the magnetic circuit are laminated silicon-iron end and center pieces in contact with the ends of the Terfenol rods. These 0.006-inch (0.15 mm) laminations were contained within the aluminum frame pieces that can be seen at the center and at the outer ends of the coils in Fig. 2a.

One of the concave aluminum shells can be seen at the right of Fig. 2a. The shell cross-section is circumscribed by a rectangular area 9.8 x 5.0 inches (250 mm x 126 mm). During assembly, the shells were elongated enough (i. e., along the long dimension) to allow insertion of the driver rod assembly through the use of a special jig that pulled on the concave surfaces. The outside length of the magnetic flux path assembly and the inside length of the shell were carefully controlled to establish a compressive prestress of 2000 psi (14 MPa) within the Terfenol rods. Two driver modules, each consisting of one shell, two coils, two Terfenol rods, and their associated magnetic flux-path pieces, were individually assembled. The completed transducer, shown in Fig. 2b, consisted of two such modules, together with the top and bottom flanges, the tie rods, and the neoprene rubber boot. (The top flange is shown at the left in Fig. 2a, while the bottom flange and the tie rods can be seen at the center of Fig. 2a.) The height of the two shells was 4.7 inches (120 mm), while the overall height (i. e., counting the flange thickness) was 5.8 inches (148 mm).

Transmitting response and impedance measurements of the projector were performed at NUWC's Seneca Lake Test Facility, with the transducer at depths ranging from 100-400 ft (30-123 m). The highest source levels were achieved at the 400-ft depth, where the ambient temperature was 4.7 C, corresponding to a sound speed of 1422 m/s. The transducer was

suspended from a spreader-bar that also supported an F-37 hydrophone at a horizontal distance of 14.6 ft (4.45 m). The 600-ft (180 m) drive cable was unshielded, with 3 AWG #10 conductors, and with two of the three conductors tied together electrically.

A simplified block diagram of the experimental arrangement is shown in Fig. 3. The projector was driven by a Ling water-cooled, vacuum-tube, 175-kVA power amplifier. The ac voltage, current, and sound pressure levels were all measured, recorded, and displayed by a computer-based, digital system developed for use at Seneca Lake by Arthur Treisback. The same system generated the input tone bursts with frequencies that were varied from 500 Hz to 1400 Hz (in 10-Hz steps) for these measurements. The ac drive current, held constant during a frequency sweep, was pulsed (13 ms pulses at the rate of 1 pulse per second) and measured with a Pearson 10-mV/A current transformer. Measurement of the bias current required the use of a 0.1-Ohm, 250-W sampling resistor in series with the projector. This sampling resistor also provided a check on the ac drive current measurement at the lower drive levels.

To minimize heating of the transducer, the bias current was pulsed. The input ac tone bursts were combined with the synchronized, dc pulses in a summing network. Then, an equalizer circuit boosted the low-frequency portion of the combined pulse (to compensate for the rolloff of the output power transformer below 300 Hz) so that the output current consisted of a bias pedestal plus an ac tone burst. The internal temperature of the projector was monitored via thermistors attached to two of the drive coils.

The resonance frequency, f_0, was determined as the frequency of maximum resistance and transmitting current response, TCR. (We are assuming negligible eddy current losses and directivity; otherwise the peak values of resistance and/or TCR could be skewed toward higher frequencies.) To determine the optimum bias current, the TCR was measured as a function of frequency for constant drive and bias currents. The resonance frequency and the maximum TCR, occurring at resonance, were noted for various bias levels. The optimum bias current was considered to be that yielding the largest TCR and the lowest resonance frequency.

Measurements were conducted of the electrical impedance with the transducer suspended in air to determine the effective coupling factor. For these measurements, an Analogue-Techron 7715 dc power amplifier was used to drive the projector. The bias current for the air-loaded case was determined as that bias current yielding the minimum resonance frequency and the maximum resistance at resonance. The coupling factor was determined from the impedance magnitude method described in Ref. 14.

III. RESULTS AND DISCUSSION

A. Bias conditions

Table I lists the measured optimum bias current, i_0, for the transducer in air and in water at depths of 100, 200, and 400 ft. The magnetic field strength corresponding to these bias currents was estimated from the relationship for a long solenoid,

$$H_0 = ni_0/4\, l_{coil}\,, \tag{19}$$

where n is the number of turns, 489, per coil, and l_{coil} is the coil length, 69.0 mm. It can be seen (in Table I) that i_0 and H_0 are both strong functions of the operating depth. This stems from a corresponding variation in the Terfenol-rod compressive prestress.[7,8] Finite-element calculations of the compressive prestress yielded

$$T_0 = -(2000 + 10.2\ d) \quad \text{psi} \tag{20}$$

where d is the water depth in feet, and these values are given in Table I, along with the expected values of the bias field from Ref. 8. There is good agreement between the expected and measured values at 200 and 400 ft, but under the lower prestress conditions at 100 ft and in air, the bias fields tend to be higher than those recommended in Ref. 8.

Table I. Prestress, T_0, calculated from finite-element results (Eq. (20)), as a function of depth. Optimum bias current, i_0, and estimated magnetic field strength, H_0, (from Eq. (19)) compared with the expected field strength from Ref. 8.

Depth (ft)	$-T_0$ (psi)	$-T_0$ (MPa)	i_0 (A)	H_0 (Oe) Eq. (19)	H_0 (Oe) Ref. 8
0 (air)	2000	13.8	22.5	500	345
100	3020	20.8	32	712	598
200	4040	27.8	40	889	851
400	6080	41.9	63	1400	1360

B. Projector performance

The source level obtained from the projector at the 400-ft depth is plotted in Fig. 4 for various ac drive levels. The maximum source level, 212 dB//μPa-m at a resonance frequency of 930 Hz, was achieved with a drive current of 50 A rms. The source level of 212 dB//μPa-m represents an omnidirectional acoustic power of 14.1 kW. (Although no beam patterns were measured during our experimentation with this particular transducer, beam patterns obtained for a scaled, permanent magnet-biased transducer of identical shape[20] were omnidirectional up to frequencies corresponding to 1200 Hz for our projector.)

With a mass of 15.4 kg (in air), the Terfenol projector had a power density of 917 W/kg, an order of magnitude greater than that obtainable from piezoeceramic-based flextensional transducers driven at their long-term, electric-field limit[21] of 10 kV/inch (about 400 kV/m) rms. Figure 5 compares the power density of our Terfenol projector (solid curve) with two high power, Class IV (oval), flextensional transducers that utilize PZT as the transduction material. These two are 1) a Sanders Model 30 projector, capable of 207.5 dB//μPa-m at 1030 Hz and weighing 43 kg, and 2) a British Aerospace Model WA316, with a mass of 89 kg, which produces 206.2 dB//μPa-m at 813 Hz.

The mechanical storage factor, Q_m, measured from the 3-dB-down width of the TCR, was 4.72, and so a projector figure of merit, defined as the radiated power per (mass-frequency-Q_m), was 14,100/(15.4 x 0.93 x 4.72) = 209 W/kg-kHz-Q. This number is comparable to the highest levels achieved by any high-power projector known to the authors at the present time.

The reactance, X, and the resistance, R, are plotted in Fig. 6 for the 50-A drive condition. At resonance, the values were 14.6 and 10.9 Ohms, respectively. The input ac power was then $10.9 \times (50)^2 = 27.2$ kW, and so the ac electroacoustic efficiency, η_{ea}, was 52 percent. For a dc-biased transducer, power is required to provide the bias field, and with the 1.0-Ohm dc resistance of the transducer plus its cable, the dc power was 4.0 kW. Thus the overall (dc + ac) efficiency was about 45 percent. This compares unfavorably with efficiencies, on the order of 80 percent, routinely obtained nowadays with piezoceramic transducers. The latter owe the bulk of their losses to mechanical inefficiencies, and magnetostrictive transducers can be expected to have comparable mechanical losses. In the present case, the mechano-acoustic efficiency, η_{ma} was about 90 percent, and so there is little to be gained by mechanical improvements in this transducer.

On the other hand, the electromechanical efficiency, η_{em} was about 57 percent, whereas the corresponding value for piezoelectric projectors is near 100 percent. Such electrical losses, due to eddy currents and other unavoidable ac resistances, are to be expected to persist in magnetostrictive transducers. Although the Terfenol rod laminations were thin (0.14 inch) enough to preclude significant eddy current losses within the rods (the critical frequency was calculated to be about 10 kHz, well above the frequencies of operation), a number of the laminations were found to be electrically shorted when tested with a dc ohmmeter, suggesting room for improvement in the lamination process.

The coupling factor, measured in air, was about 29 percent. This is somewhat lower than typical values (about 35 percent) achieved in good piezoceramic flextensional transducers.[22] The material coupling factors of PZT and Terfenol are comparable (both are about 0.7), and so the lower present value is not a result of a lower material coupling factor. Furthermore, the mechanical assembly procedures were quite similar to those required of high quality piezoelectric transducer construction, and so mechanical causes of the reduced coupling are not to be expected. (The shape of the shell is different from the traditional, Class IV oval shape, and if it had been built as illustrated in the Merchant[4] patent, with end walls no thicker than the side walls, end flexure could have resulted in lower effective coupling.) The lower coupling (i. e., 29 percent instead of 35 percent) is probably due to magnetic field leakage. The coils cannot couple all of their magnetomotive force into the Terfenol rods because of the low permeability of Terfenol and because the coils are necessarily larger in diameter than the Terfenol rods, leaving an annular space in which magnetic fields are generated, but not used.

C. Equivalent circuit parameters

We can now follow the procedure outlined in Sec. I to obtain the equivalent circuit parameters. With the (open-circuit) resonance frequency, f_0, of 930 Hz and the blocked reactance, X_b, measured at f_0, of 14.6 Ohms, the blocked inductance, from Eq. (14), is

$$L_b = 2.49 \text{ mH} .$$

From the coupling factor, k, of 0.29, and the use of Eq. (18), the motional inductance, is

$$L_m = 0.23 \text{ mH} .$$

From the 930-Hz resonance frequency, f_0, and Eq. (13), we obtain the motional capacitance,

$$C_m = 130\ \mu F\ .$$

Measurement of the mechanical quality factor, $Q_m = 4.72$ (as $f_0/(f_2 - f_1)$, where f_2 and f_1 are the quadrantal, or half-power, frequencies), yields

$$G_r + G_m = 0.160\ \text{Mho}\ ,$$

with the help of Eq. (12). From this result and the measured value of the resistance at resonance, we can extract the blocked resistance, R_b, using Eq. (15):

$$R_b = 4.63\ \text{Ohms}\ .$$

Next, the electromechanical efficiency, η_{em}, as determined via Eq. (16), turns out to be 0.574. Then, the measured electroacoustic efficiency, η_{ea}, 0.515, and Eq.(17) may be used to determine the mechanoacoustic efficiency, $\eta_{ma} = 0.898$. The latter quantity and Eq. (11) determine the motional radiation conductance, $G_r = 0.144$ Mho. Finally, one obtains the motional loss conductance, $G_m = 0.016$, from the previously determined values of G_r and $(G_r + G_m)$.

At this point, we have determined the elements comprising the equivalent electrical circuit of Fig. 1b. The electromechanical elements of Fig. 1a are obtained by initial substitution of the transducer radiating area, A, estimated to be 0.109 m^2, into Eq. (1), with the result for the radiation resistance,

$$R_r = 22.7\ \text{kN-s/m}\ .$$

The electromechanical gyrator ratio is then determined from Eq. (10) as

$$\gamma = 397\ \text{N/A}\ .$$

Then, from Eq. (9), the mechanical loss resistance is

$$R_m = 2.57\ \text{kN-s/m}\ ,$$

while, from Eq. (8), the mass is

$$M = 20.4\ \text{kg}\ ,$$

and from Eq. (7), the open-circuit compliance is

$$C_m^I = 1.43\ \text{nm/N}\ .$$

D. Other considerations

The breathing mode resonance occurred at approximately 3 kHz at the 400-ft operating depth, i. e., about three times the fundamental, flextensional resonance. At this frequency, the beam patttern is expected to be noticeably directional because the transducer length is comparable to

one-half wavelength, and because the motion of the shell ends is out of phase with that of the side walls, giving rise to a quadrupole source distribution.

The harmonic distortion of the acoustic waveform was relatively high, about 26 percent at the maximum drive level of 50 A rms. Since the peak value corresponding to 50 A is 71A, and the bias current was only 63 A, the Terfenol rods were being driven past zero by about 10 percent at this high drive level, and the drive current harmonic distortion was indeed measured to be 10 percent. One would expect the distortion of the output waveform to increase rapidly at this point. At the lower drive level of 20 A rms, the measured output and input distortion percentages were 12 and 7, respectively.

IV. CONCLUSIONS AND RECOMMENDATIONS

Our experimental results with the Terfenol-D flextensional projector indicate that high-power transducers with reasonable coupling and efficiency can be designed and constructed. The increase in radiated power density, over that of PZT-based flextensional transducers, comes at the expense of reduced efficiency and reduced coupling, but these are prices one might be willing to pay in order to obtain higher source levels from smaller source volumes and masses.

If the projector operation were to be primarily at a single design depth, permanent-magnet biasing would be preferred over the dc biasing method used in the present instance, because no power would be required to establish the bias field. For variable depth applications, however, the compressive prestress on the Terfenol rods becomes a strong function of depth, and that means that the optimum bias field is also strongly depth-dependent. The variation in bias field, a factor of two as the depth was changed from 100 ft to 400 ft in our case, could not have been accomplished with permanent magnets. For high power drive conditions, the dc-bias power required is small compared to the acoustic power radiated (4 kW vs 14 kW in our case).

A further argument for the use of dc-biasing is that the magnetic return path has a lower reluctance than that necessitated by the presence of permanent magnets. High-energy-product permanent-magnet materials have a permeability nearly equal to that of free space. Thus, magnets behave as if there were a series of air gaps within the magnetic return loop, and so excess ac magnetomotive force (i. e., excess drive current) would be required to produce a given drive field within the magnetostrictive rods. The effective coupling factor of a transducer containing permanent magnets would therefore be smaller than for one utilizing dc biasing.

To avoid heating the transducer, the dc bias current should be pulsed, as is the radiated underwater sound. (Only if continuous high power is required from an underwater projector would permanent-magnet biasing be preferred.) This requirement puts a burden on the power amplifier, which now must be capable of handling both the dc pedestal pulse and the ac tone burst, but this does not appear to be an insurmountable problem.

ACKNOWLEDGMENTS

The authors are indebted to A. E. Clark (NSWC) and J. F. Lindberg (NUWC) for their encouragement and support. J. L. Butler (Image Acoustics) suggested that the Class IV flextensional geometry was better suited to Terfenol than the barrel-stave flextensional

flextensional configuration. Valuable design inputs were provided by W. L. Clay, Jr., and J. M. Powers (both of NUWC Detachment New London). Finite-element mechanical modeling was performed by C. Wason and P. Harvey (both of Lockheed-Sanders), while magnetic-field modeling was done by W. Harrold (Image Acoustics) and J. Restorff (NSWC). The initial computer-aided drafting was by P. Dell'Erba, J. Polan, and J. Wiley (all NUWC). The manufacture of the Terfenol-D rods was overseen by D. McMasters (Etrema Products). The drive waveform-shaping electronics was designed by S. Gilardi (Interface Engineering). A. Treisback (Analysis and Technology) and M. F. Debolt (NUWC Seneca Lake) provided vital experimental assistance at Seneca Lake, and C. Wyatt (NUWC Detachment New London) assisted with the coupling factor measurement. Experimental data on the Sanders Model 30 and British Aerospace transducers were provided, respectively, by R. S. Janus and M. E. Werbicki (both of NUWC Detachment New London).

REFERENCES

1. K. D. Rolt, "History of the flextensional electroacoustic transducer," J. Acoust. Soc. Am. **87**, 1340-1349 (1990).

2. L. H. Royster, "The flextensional concept: a new approach to the design of underwater acoustic transducers," in **Applied Acoustics** (Elsevier, London, 1970), pp. 117-126.

3. R. L. Smith, "Evaluation of stress-induced depolarization of PZT-8 ceramic," TRI Rept. A7407-105:RLS-D187.5 (Texas Research Institute Austin, August, 1994).

4. H. C. Merchant, "Underwater transducer apparatus," U. S. Patent No. 3,258,738 (28 June, 1966).

5. E. F. Rynne, "Innovative approaches for generating high power, low frequency sound," in **Transducers for Sonics and Ultrasonics**, ed. by M. D. McCollum, B. F. Hamonic, and O. B. Wilson (Technomic, Lancaster, PA, 1993), pp. 38-49.

6. R. Porzio, W. J. Harrold, and J. R. Sturges, "Self-biased modular magnetostrictive driver and transducer," U. S. Patent No. 4,845,450 (4 July, 1989).

7. M. B. Moffett, A. E. Clark, M. Wun-Fogle, J. F. Lindberg, J. P. Teter, and E. A. McLaughlin, "Characterization of Terfenol-D for magnetostrictive transducers," J. Acoust. Soc. Am. **89**, 1448-1455 (1991).

8. M. B. Moffett, J. M. Powers, and A. E. Clark, "Comparison of Terfenol-D and PZT-4 power limitations," J. Acoust. Soc. Am. **90**, 1184-1185 (1991).

9. M. B. Moffett and W. L. Clay, Jr., "Demonstration of the power-handling capability of Terfenol-D," J. Acoust. Soc. Am. **93**, 1653-1654 (1993).

10. J. L. Butler, M. B. Moffett, and K. D. Rolt, "A finite element method for estimating the effective coupling coefficient of magnetostrictive transducers," J. Acoust. Soc. Am. **95**, 2533-2534 (1994).

11. G. A. Brigham, "Lumped-parameter analysis of the Class-IV (oval) flextensional transducer," NUSC Technical Report 4463 (Naval Underwater Systems Center, New London, CT, 15 August 1973).

12. J. L. Butler, "A computer program for the Class IV flextensional transducer," Final Report, Contract N00140-85-M-LK94 (Image Acoustics, Marshfield MA, 15 July 1985).

13. M. B. Moffett, J. F. Lindberg, E. A. McLaughlin, and J. M. Powers, "An equivalent circuit model for barrel-stave flextensional transducers," in **Transducers for Sonics and Ultrasonics** , ed. by M. D. McCollum, B. F. Hamonic, and O. B. Wilson (Technomic, Lancaster, PA, 1993), pp. 170-180.

14. R. S. Woollett, "Effective coupling factor of single-degree-of-freedom transducers," J. Acoust. Soc. Am. **40**, 1112-1123 (1966).

15. K. S. Van Dyke, "The piezoelectric resonator and its equivalent network," Proc. IRE, **16**, 742-764 (1928).

16. R. S. Woollett, **The Flexural Bar Transducer**, ed. by L. C. Maples (Naval Underwater Systems Center, New London, CT, 1986), p. 14.

17. R. S. Woollett, Sec.1, "General transducer theory," in **Sonar Transducer Fundamentals**, ed. by D. T. Porter (Naval Underwater Systems Center, New London, CT, 1990), p. 18.

18. D. A. Berlincourt, D. R. Curran, and H. Jaffe, "Piezoelectric and Piezomagnetic Materials and Their Function in Transducers," in **Physical Acoustics: Principles and Methods, Vol. I - Part A**, W. P. Mason, ed. (Academic, New York, 1964).

19. D. Stansfield, **Underwater Acoustic Transducers: A Handbook for Users and Designers** (Bath Univ. Press and Inst. of Acoust., Bath, UK, 1990).

20. D. F. Jones and J. F. Lindberg, "Recent transduction developments in Canada and the United States," Proc. of the Inst. of Acoust.: Sonar Transducers '95, Univ. of Birmingham, UK, 3-5 April 1995.

21. R. S. Woollett, "Power limitations of sonic transducers," IEEE Trans. Sonics Ultrason. **SU-15**, 218-229 (1968).

22. W. J. Marshall, Jr., private communication to one of the authors (MBM).

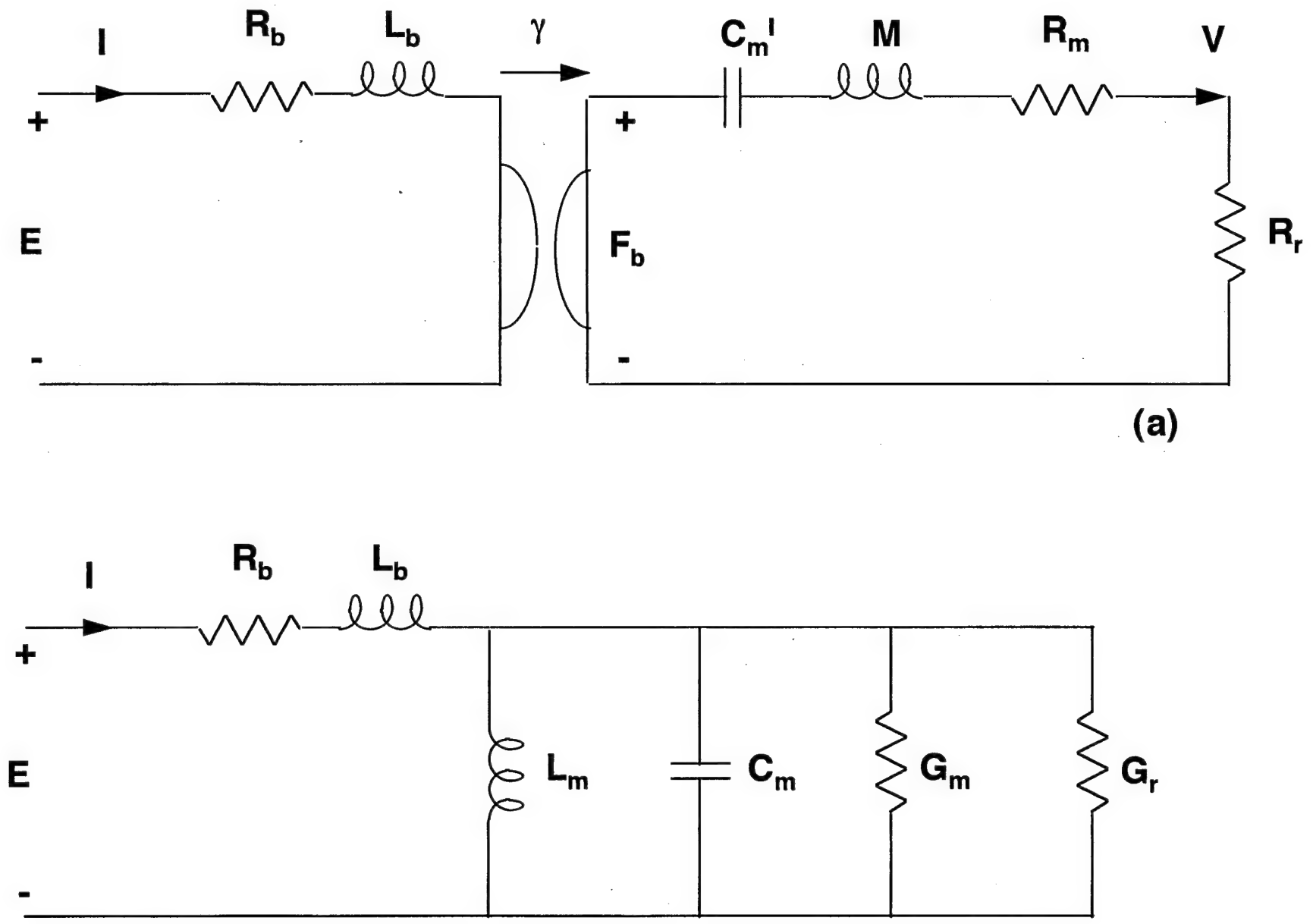

Fig. 1. Canonical equivalent circuit for magnetostrictive projector, (a) with mechanical loop as impedance analogy, and (b) with motional electrical branch in place of mechanical loop.

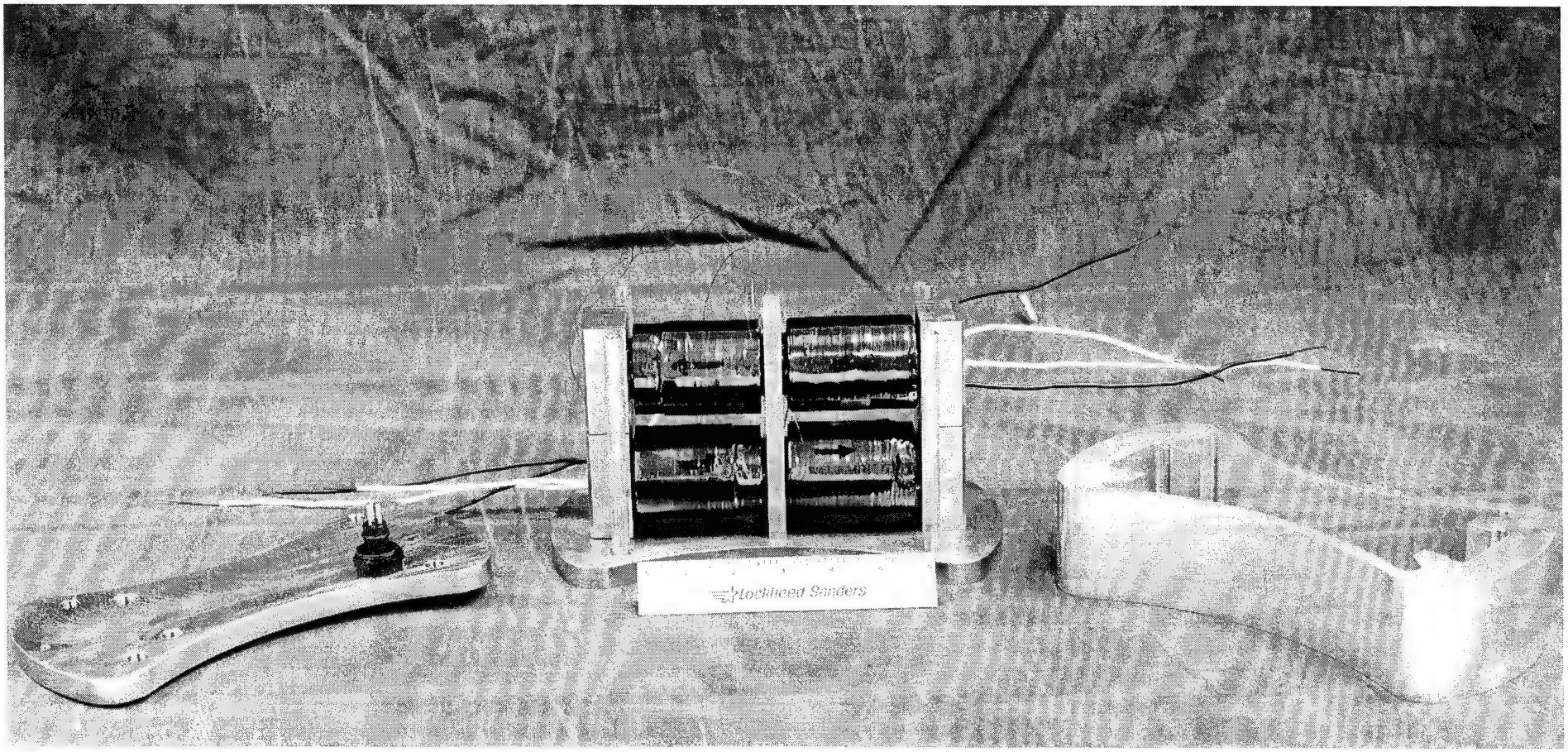

Fig. 2a. Photographs of Terfenol-D flextensional projector: (left) top flange; (center) coils, magnetic flux return path support pieces, bottom flange, and tie rods; (right) shell;

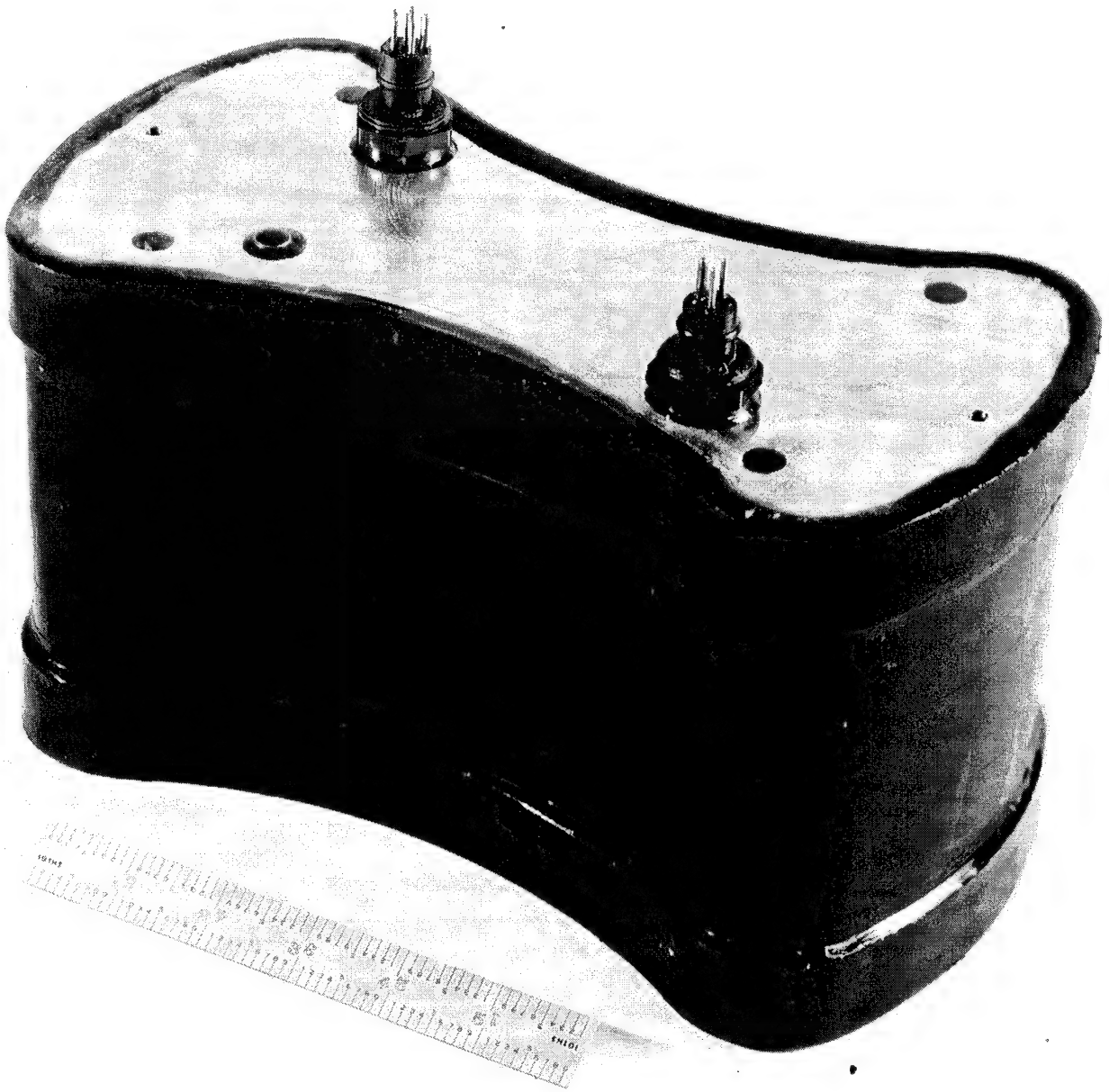

Fig. 2b. Photograph of Terfenol-D flextensional projector: completed assembly.

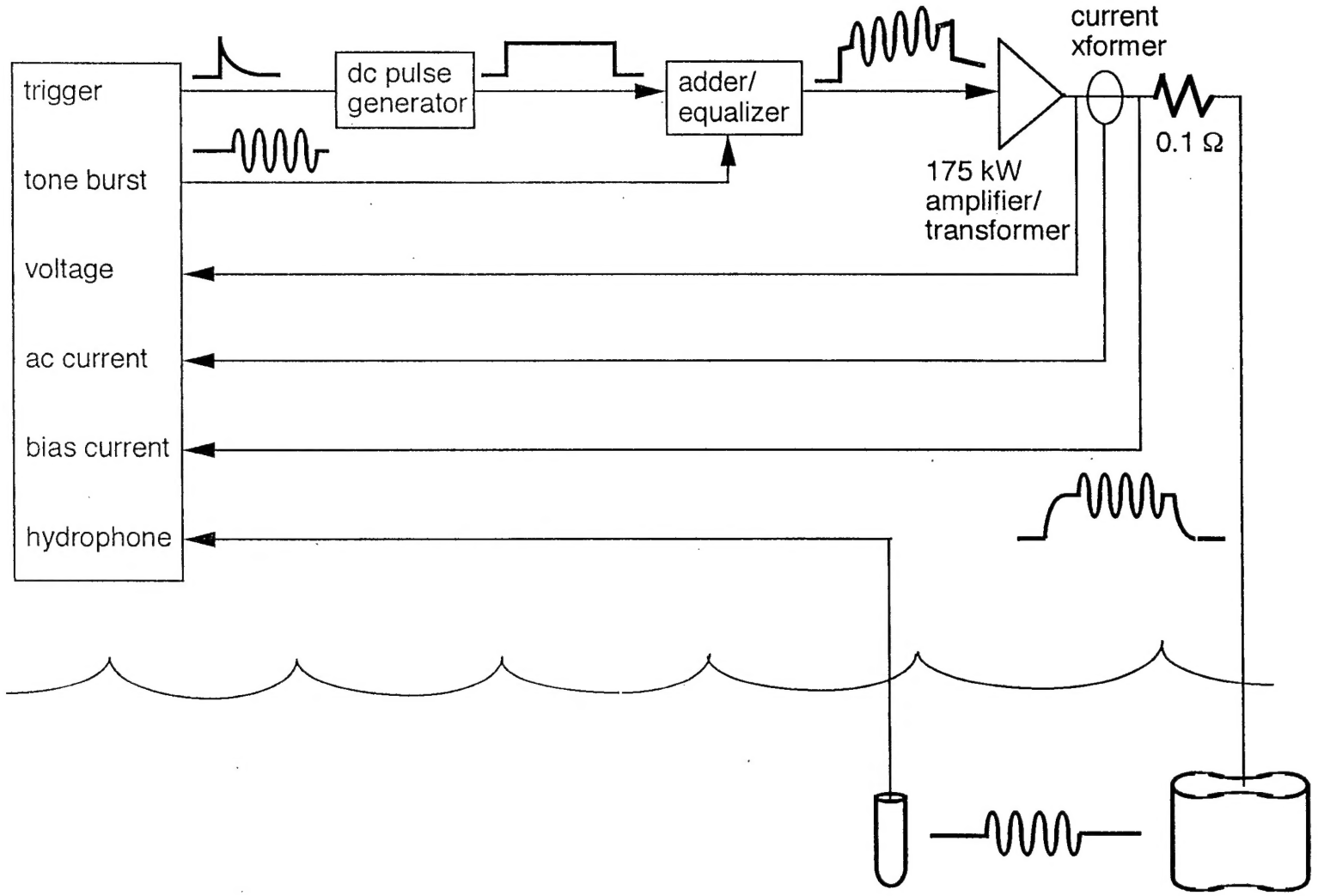

Fig. 3. Simplified block diagram of experimental arrangement.

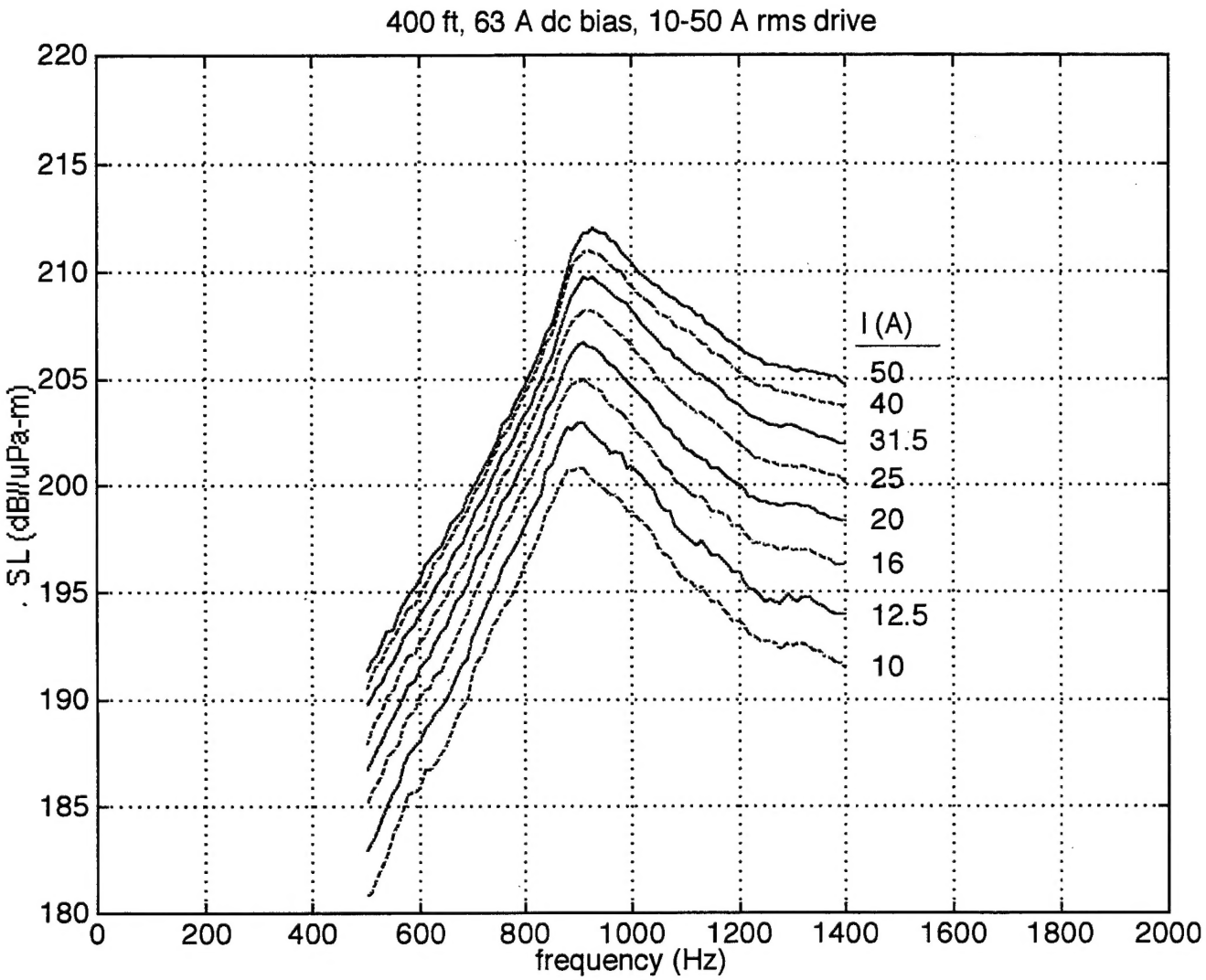

Fig. 4. Source level at 400-ft operating depth for drive currents from 10 to 50 A rms.

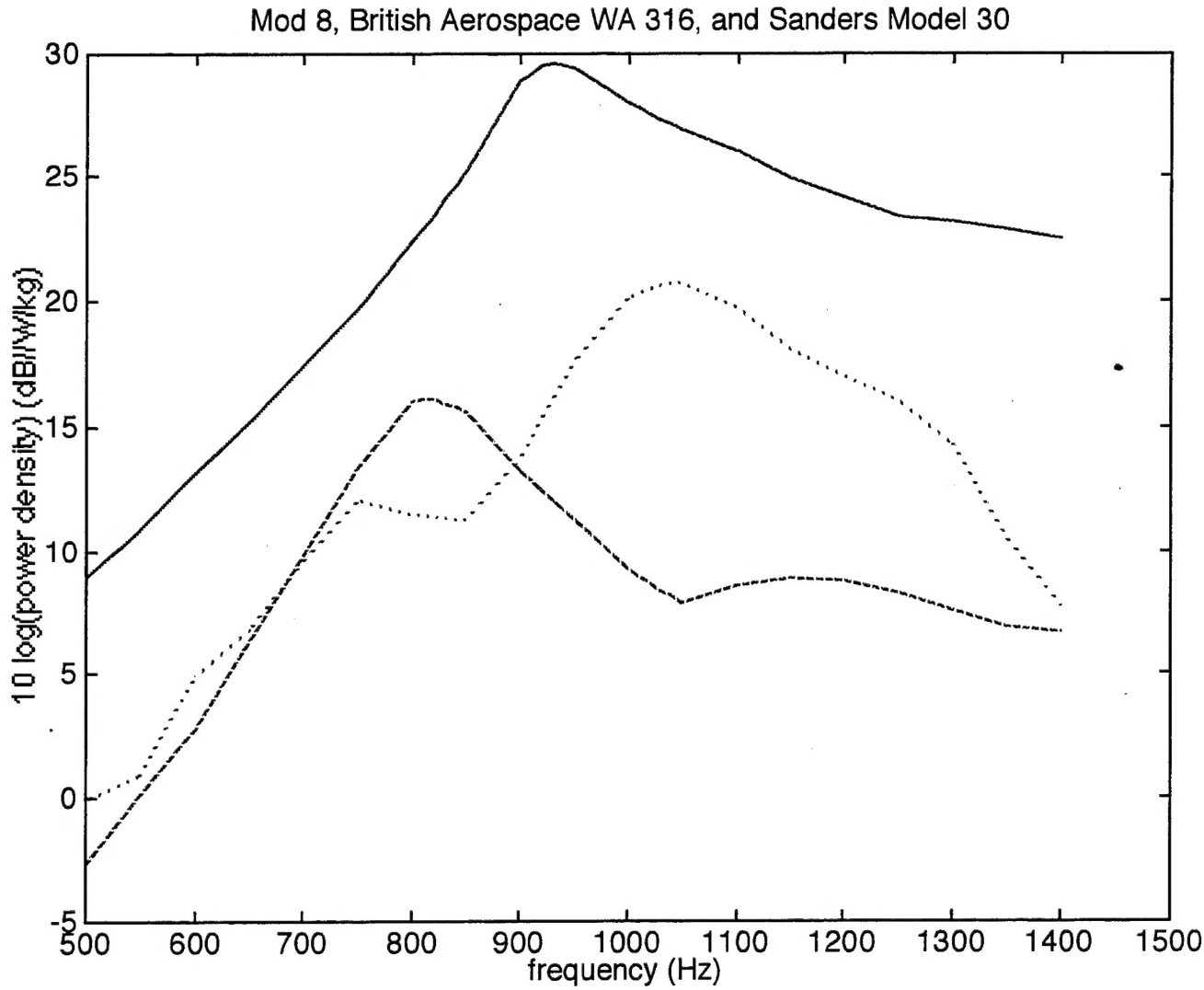

Fig. 5. 10 log (power/mass) versus frequency for three flextensional projectors: Terfenol Class VII (solid curve), Sanders Model 30 (short dashes), and British Aerospace Model WA 316 (long dashes).

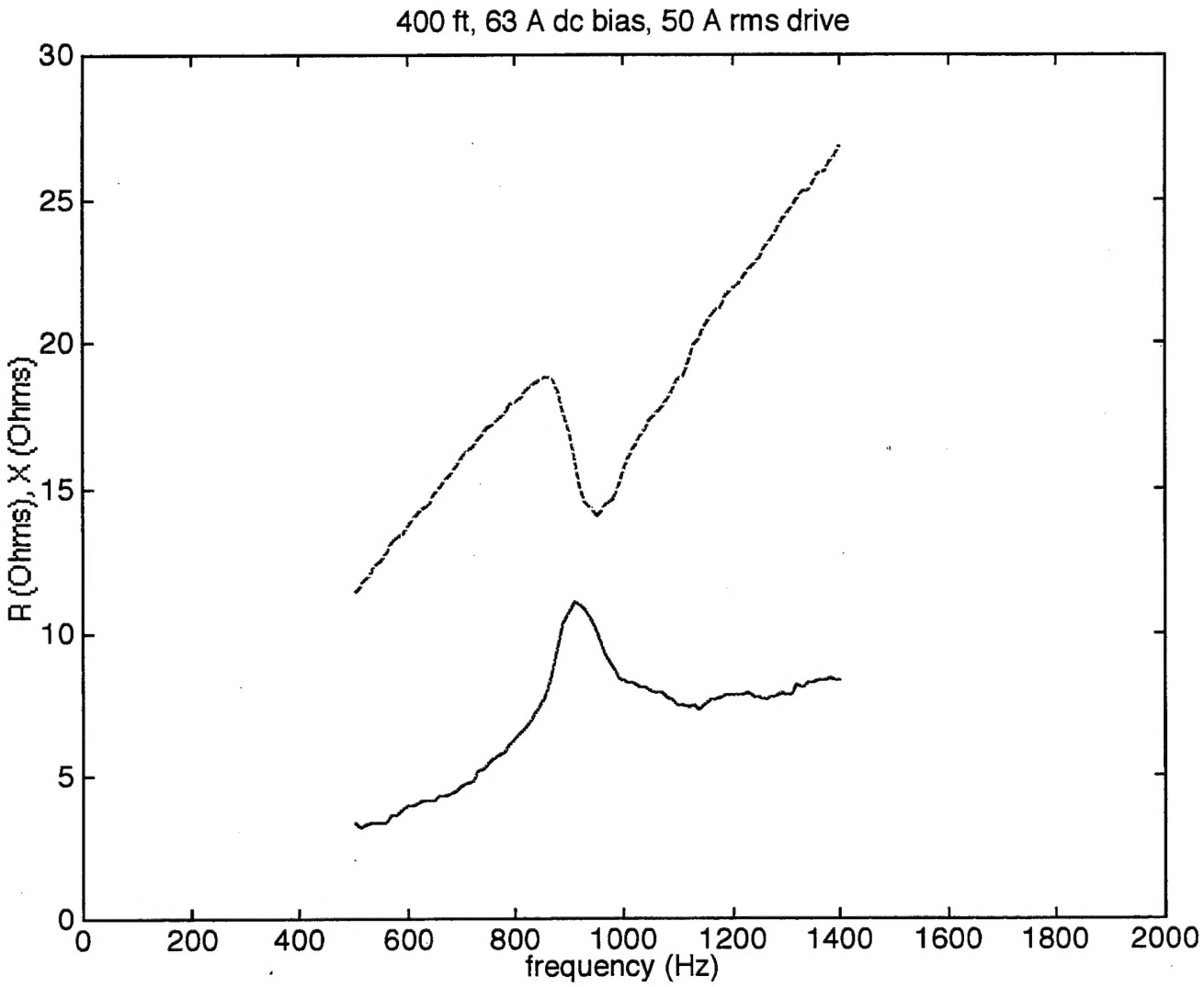

Fig. 6. Reactance, X (upper curve), and resistance, R (lower curve), at 400-ft operating depth and 50-A rms drive current.